

Guiding of highly charged ions by highly ordered SiO₂ nanocapillaries

M. B. Sahana,* P. Skog, Gy. Viktor, R. T. Rajendra Kumar, and R. Schuch

Atomic Physics, Fysikum, AlbaNova, S-10691 Stockholm, Sweden

(Received 17 January 2006; published 26 April 2006)

We report a narrow angular distribution of 0.8°, close to that expected from the aspect ratio, for guiding of highly charged ions through a well-ordered, parallel SiO₂ nanocapillaries target. These capillaries were obtained by thermally oxidizing a 25- μm -thick membrane of silicon nanocapillaries fabricated by photoassisted electrochemical etching. The diameter of the uniformly distributed capillaries was 100 nm. We observed Ne⁷⁺ ions being transmitted through these nanocapillaries with a decreasing transmitted intensity up to a factor 100, when increasing the capillary tilt angles up to 4°. The narrower angular distribution in comparison to polyethylene terephthalate capillaries is discussed and it is shown that the SiO₂ results support the model of self-organized charge patches formed at the capillary entrance.

DOI: [10.1103/PhysRevA.73.040901](https://doi.org/10.1103/PhysRevA.73.040901)

PACS number(s): 79.20.Rf, 34.50.Dy, 81.07.De

The transmission of highly charged ions (HCI) through nanocapillaries has attracted considerable attention during recent years [1–6]. It offers the possibility of manipulating HCI in the nanoscale for controlled surface modifications. It was found that HCI are transmitted through metallic capillaries only at angles corresponding to the capillary aspect ratio. They can capture several electrons, resulting in hollow atom formation [1,3], when approaching the capillary walls within the critical distance. Recently, Stolterfoht *et al.* [2] reported transmission of 3 keV Ne⁷⁺ through insulating nanocapillaries of polyethylene terephthalate (PET) with angular widths much larger than those given by the aspect ratio. Substantial ion transmission up to the capillary tilt angle of 25° with respect to the incident HCI beam, without changing the initial ion charge state and energy, was observed. This revealed the significant difference in the phenomena involved in the transmission of HCI through metallic and insulating nanocapillaries, which must be due to the different electrical properties of the walls of the capillaries.

In contrast to metallic capillaries, the angular distributions of the ions transmitted through insulating PET capillaries were much broader ($\approx 5^\circ$ for 3 keV and 2.9°–3.2° for 7 keV Ne⁷⁺ ions) than those given by the aspect ratio [1,2,5,7]. In the first model of HCI guiding through the insulating nanocapillaries [8], the guiding effects were attributed to self-organized charge-up effects that inhibit HCI from hitting the capillary walls, thus transmitting large fractions of ions in the incident charge state. The measured broad angular distributions suggested an array of multiple charge patches, alternating on opposite sides of the capillary walls. Recently, numerical simulations by Schiessl *et al.* [6,9] showed that multiple patch arrays are not stable and that the angular spread of the transmitted beam should be close to the value given by the aspect ratio. The model does not give good agreement with the charging up and discharging times found in the experiments. Even though there are attempts to explain

these phenomena by taking nonlinearity in the charge transport into consideration, ion guiding through insulating nanocapillaries is not well understood [8,9].

An uncertainty comes from the geometrical properties of the capillaries in PET. They are randomly distributed and have irregular shapes (diameters of about 100 \pm 20 nm), as they are fabricated by etching random ion tracks in 10- μm -thick PET foil. The PET nanocapillaries' axes have an angular width of 2° [5] and in some places of the foil the capillaries are aggregated. To avoid the geometrical anomalies present in PET capillaries (due to the production method), we fabricated highly ordered, parallel Si nanocapillaries by making use of optical lithography and photoassisted electrochemical etching. With this method we were able to obtain capillaries of different lengths, openings, and pitch (distance between the capillaries). Dielectric properties of the walls of the capillaries are achieved by thermally oxidizing the membrane to grow a 100-nm-thick layer of silicon dioxide on the capillary walls. The diameters of the capillaries after oxidation are around 100 nm, and the lengths are 25 μm . To prevent the charging up of the target surface by the incident HCI, 30-nm-thick gold layers were evaporated on the entrance and exit side. A detailed description of the Si/SiO₂ nanocapillary fabrication is given elsewhere [10].

The experiments were carried out at the 14-GHz Electron Cyclotron Resonance Ion Source (ECRIS), located at the Manne Siegbahn Laboratory in Stockholm. ECRIS delivered Ne⁷⁺-ions with kinetic energy of 7 keV that were transported to the experimental chamber with the help of an electrostatic lens system. The nanocapillary array was mounted on a target holder of a manipulator with five degrees of freedom (three axial and two rotational), allowing the orientation of the target position with respect to the beam direction. The experimental chamber was evacuated down to 10⁻⁹ torr. An electrostatic spectrometer with an acceptance angle of 0.36° and two channeltron detectors were used for detecting the ions transmitted through the capillaries. The spectrometer scans the angular region between -3° and 13°. The angle between the capillary axis and the incident beam direction is referred to as the tilt angle in the discussion to follow. The observation angle θ is measured with respect to the incident beam direction.

*Corresponding author. Present address: Department of Physics and Astronomy, Wayne State University, Detroit, Michigan, 48201. Email address: sahanamb@yahoo.com

An average ion current density of $\approx 0.082 \pm 0.02$ nA/mm² was used for the measurements. However, the intensity of the ion beam was not uniform over the exposed area. We measured an angular spread of 0.36° without capillary target, which is equal to the spectrometer acceptance angle. This suggests that this spread is due to the resolution of the spectrometer, and the actual beam divergence is negligible. Further details of the experimental setup are given elsewhere [7].

Due to the thinness of the capillary region of the Si wafer and the differences in the lattice constants of Si and SiO₂ the surface of the capillary array region is not perfectly flat; it has a slight curvature. From the variation of transmission angle with the beam position on the membrane we estimate a curvature of 0.1° over a 100-mm² area. The highly ordered SiO₂ nanocapillaries with an intercapillary distance of $1.4 \mu\text{m}$ have a geometrical transparency of 0.4%. In the experiment we found that $\sim 20\%$ of the Ne⁷⁺ ions entering the capillaries at 0° tilt angle are being transmitted.

The observed centroid positions of the transmitted beam were approximately equal to the tilt angles as expected from a guiding effect of HCl through SiO₂ nanocapillaries. The transmitted Ne⁷⁺ intensity decreases with increasing tilt angle, setting a limit for the largest tilt angle at which we can observe this guiding phenomenon. We were able to observe the guiding of Ne⁷⁺ ions through SiO₂ nanocapillaries for capillary tilt angles of up to 4° . At this angle the transmitted intensity was 1% of the intensity at 0° .

Similar to the transmission of HCl through PET, we found that the majority of the ions transmitted through SiO₂ nanocapillaries survive in their initial charge state, Ne⁷⁺, irrespective of the tilt angle. Less than 2% of the ions transmitted through the nanocapillaries have undergone charge exchange collisions with the capillary walls.

The integrated intensities of the detected Ne⁷⁺ and Ne⁶⁺ ions are given in Fig. 1 as a function of the observation angle θ . The data were acquired for different tilt angles varying from -1° to 4° in steps of 1° , with uncertainties in the tilt angles of $\pm 0.1^\circ$ (augmented by the slight curvature of the membrane) and in the observation angles of $\pm 0.1^\circ$. The apparatus contribution to the angular spread is approximately 0.36° . Table I gives the angular spread of the transmitted beam before and after the corrections for contributions from spectrometer acceptance angle, and foil curvature. In contrast to the experiments with 7-keV Ne⁷⁺ through PET nanocapillaries [5,7,12,13], the angular distributions of the ions transmitted through SiO₂ nanocapillaries are narrower, with widths of $\sim 1^\circ$ full width at half maximum (FWHM), probably partly due to the capillary axes being parallel (neglecting the aforementioned slight curvature), as opposed to the spread of the capillary axes of the PET membranes. The narrow angular distribution supports the model of self-organized charge patches formed at the capillary entrance [6,9]. From Table I it is evident that the spread in the transmitted beam is slightly larger than the value calculated from the aspect ratio of the capillaries. This can be explained as follows. A large number of capillaries are irradiated by the incoming ions. Ions hitting the inner walls of the capillaries will deposit positive charges on the capillary walls, with the highest concentrations of deposited charge being located in

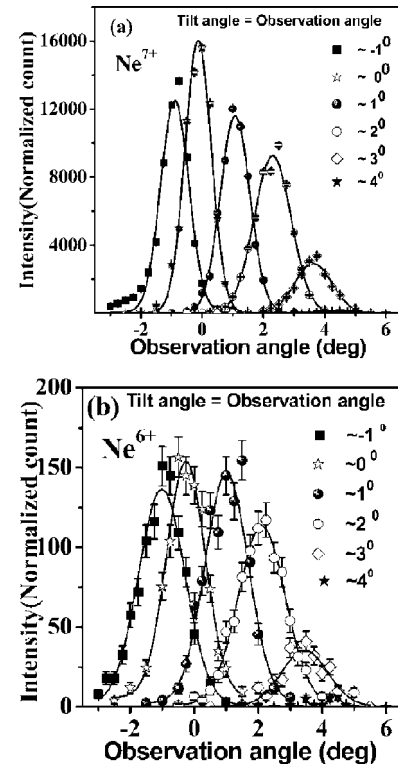


FIG. 1. Angular distributions of (a) Ne⁷⁺ and (b) Ne⁶⁺ ions transmitted through the SiO₂ nanocapillaries.

charge patches near the entrances. The array of charged-up capillaries between the two grounded gold layers, with charge patches close to the entrance surface, can be viewed as a charged condenser with small holes [6,9]. It should be noted here that the nanocapillaries are fabricated by thermally oxidizing Si capillaries. Therefore the dielectric properties of the capillary walls (≈ 100 nm thick SiO₂) will be different from the bulk of the membrane (n -doped Si), in contrast to the PET nanocapillaries. However, according to the simulations by Schiessl *et al.* [6,9], the ion transport through insulating nanocapillaries depends on the charge up and charge diffusion near the internal capillary walls. The

TABLE I. The angular spread of the transmitted beam before and after the corrections for contributions from spectrometer acceptance angle, and foil curvature.

Tilt angle	Before correction		After correction	
	FWHM of Ne ⁷⁺ (deg)	FWHM of Ne ⁶⁺ (deg)	FWHM of Ne ⁷⁺ (deg)	FWHM of Ne ⁶⁺ (deg)
-1	0.9	1.45	0.85	1.5
0	0.85	1.2	0.8	1.15
1	0.95	1.35	0.9	1.3
2	1.20	1.5	1.15	1.4
3	1	1.45	0.9	1.4
4	1.15		1.1	

mesoscopic field resulting from the charge up of the entire ensemble of capillaries depends on the total charge deposited on the capillary walls, the dielectric constant of the insulating material, and the irradiated target area. The dielectric constant of SiO_2 is 3.9, which is close to that of PET 3.3. The density of the SiO_2 nanocapillaries is approximately 10^6 mm^{-2} , which is comparable to the density of PET nanocapillaries used for the numerical simulations [6,9] as well as in Ref. [2]. We have estimated the influence the electric field from charge patches in adjacent capillaries has on an ion, and find that to be completely negligible compared to the field from the charge patch in the capillary the ion is passing through for the inter-capillary distances of our SiO_2 nanocapillaries. Even for the higher density of PET capillaries the influence from charge patches in adjacent capillaries, using an average intercapillary distance calculated from the geometrical transparency, can be neglected. The mean field on the exit side will converge to a homogenous field as the distance from the capillary surface goes to infinity. However, outside the capillaries, close to the exit surface of the capillaries, the mean field of all the charged-up capillaries will be inhomogeneous [6,9]. The electric-field components perpendicular to the capillary axes will deflect the ions upon their exit, thereby broadening the distribution. Hence, the resulting field close to the exit of the capillaries leads to the deflection of the transmitted projectiles. It is therefore expected that the mesoscopic charge up of the capillaries will contribute to the angular spread. Recent simulations [6,9] for PET nanocapillaries reveal that the mesoscopic charge-up contribution to the angular spread will be less than 1° .

The width of the 7-keV Ne^{7+} ions transmitted through PET, when corrected for the contribution from the distribution of the capillary axes, is 2.2° [5], which is larger than the transmitted width for the SiO_2 capillaries by more than a factor of 2. The bulk resistivity of SiO_2 is $10^{16} \Omega \text{ cm}$, while the bulk resistivity of PET is larger by two orders of magnitude. The smaller bulk resistivity of SiO_2 leads to faster diffusion of deposited charge, thereby reducing the gradient of the defocusing field at the exit; this could be the explanation for the narrower angular distribution of ions transmitted through SiO_2 capillaries compared to PET.

With that hypothesis it is very interesting to note that the angular spread obtained from the PET simulations [6,9] ($\leq 1^\circ$) is closely matching the angular spread (0.8°) for SiO_2 nanocapillaries. However, further simulations on PET and SiO_2 nanocapillaries are needed for comparison with our experimental findings.

Except for the 4° tilt angle (where statistical errors are large), the FWHM of the transmitted beam is smaller for Ne^{7+} compared to Ne^{6+} , with no significant trend in the FWHM dependence on the tilt angle (Fig. 2). According to the model proposed by Stolterfoht *et al.* the angular width is proportional to $\sqrt{q_f/E_p}$, where q_f is the final charge state and E_p is the projectile's kinetic energy [11,12]. In this model it is assumed that the main part of the transmitted ions that have undergone charge exchange have done so in the first part of the capillaries, the scattering region. Our measurements, however, show a broader distribution for $q_f=6$ than for $q_f=7$ (see Table I). Furthermore, even for HCI through PET nanocapillaries, it is reported [12,13] that the angular

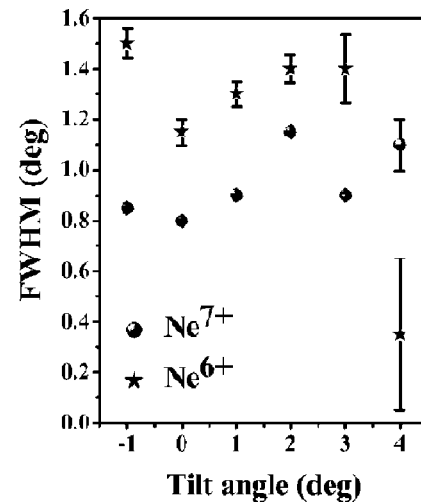


FIG. 2. Variation of angular spread of the transmitted beam intensity with respect to the capillary orientation.

spread is narrower for Ne^{7+} , compared to Ne^{6+} and Ne^{5+} . A possible explanation for this is that, for $q_f < 7$, a larger fraction of the ions is lost on their way to the exit end due to the lower charge of these ions. Therefore lower charge state ions experience their final deflection closer to the exit compared to ions with $q_f=7$, leading to a broader angular distribution. Also, the defocusing effect is stronger for ions emerging from the capillaries close to the capillary walls due to the steeper gradient of the potential there [9]. The $q_f=7$ ions that pass the exit gold layer within the critical distance will capture an electron [14], lowering the charge state, thereby broadening the distribution of the $q=6$ charge state.

In summary, our studies of transmission of HCI through highly ordered SiO_2 nanocapillaries revealed some interesting phenomena. The insulating capillaries charge up and form self-arranged ion guiding, bending keV ion beams uniformly by a few degrees without changing their charge or energy. The angular distribution of the guided beam is very narrow, close to the value given by the capillary geometrical aspect ratio, and broadened by the inhomogeneous electric field at the exit surface. This finding is quite different from the results with PET capillaries [1,2,5,7], which can partly be explained by the capillaries in SiO_2 being parallel to a high degree, together with the bulk resistivities of SiO_2 and PET that differ by two orders of magnitude. The narrow angular distribution of the ions transmitted through the SiO_2 nanocapillaries can be plausibly understood from the capillary geometrical aspect ratio and the contributions from the mesoscopic charge up of the target material. One could use this feature to develop HCI focusing elements based on the guiding effect of insulator capillaries, or to investigate and characterize the electric properties of the nanocapillary walls.

The authors would like to thank the staff of the Manne Siegbahn Laboratory (MSL) for providing the beam, and the Swedish Research Council (VR) for financial support. Two of the authors (M.B.S. and R.T.R.K.) gratefully acknowledge the European R&D network HITRAP (Contract No. HPRI CT 2001 50036) for their support.

- [1] S. Ninomiya, Y. Yamazaki, F. Koike, H. Masuda, T. Azuma, K. Komaki, K. Kuroki, and M. Sekiguchi, *Phys. Rev. Lett.* **78**, 4557 (1997).
- [2] N. Stolterfoht, J.-H. Bremer, V. Hoffmann, R. Hellhammer, D. Fink, A. Petrov, and B. Sulik, *Phys. Rev. Lett.* **88**, 133201 (2002).
- [3] K. Tokesi, L. Wirtz, C. Lemell, and J. Burgdorfer, *Phys. Rev. A* **64**, 042902 (2001).
- [4] K. Tokesi, L. Wirtz, C. Lemell, and J. Burgdorfer, *Phys. Rev. A* **61**, 020901(R) (2000).
- [5] R. Hellhammer, Z. D. Pesic, P. Sobocinski, D. Fink, J. Bundesmann, and N. Stolterfoht, *Nucl. Instrum. Methods Phys. Res. B* **233**, 213 (2005).
- [6] K. Schiessl, W. Palfinger, K. Tokesi, H. Nowotny, C. Lemell, and J. Burgdorfer, *Phys. Rev. A* **72**, 062902 (2005).
- [7] Gy. Vıkor, R. T. Rajendra Kumar, Z. D. Peřiĉ, N. Stolterfoht, and R. Schuch, *Nucl. Instrum. Methods Phys. Res. B* **233**, 218 (2005).
- [8] N. Stolterfoht, R. Hellhammer, Z. D. Peřiĉ, V. Hoffmann, J. Bundesmann, A. Petrov, D. Fink, and B. Sulik, *Vacuum* **73**, 31 (2004).
- [9] K. Schiessl, W. Palfinger, C. Lemell, and J. Burgdřrfer, *Nucl. Instrum. Methods Phys. Res. B* **232**, 228 (2005).
- [10] R. T. Rajendra Kumar, X. Badel, G. Vıkor, J. Linnros, and R. Schuch, *Nanotechnology* **16**, 1697 (2005).
- [11] N. Stolterfoht, R. Hellhammer, Z. D. Peřiĉ, V. Hoffmann, J. Bundesmann, A. Petrov, D. Fink, B. Sulik, M. Shah, K. Dunn, J. Pedregosa, and R. W. McCullough, *Nucl. Instrum. Methods Phys. Res. B* **225**, 169 (2004).
- [12] N. Stolterfoht, V. Hoffmann, R. Hellhammer, Z. D. Peřiĉ, D. Fink, A. Petrov, and B. Sulik, *Nucl. Instrum. Methods Phys. Res. B* **203**, 246 (2003).
- [13] R. Hellhammer, P. Sobocinski, Z. D. Peřiĉ, J. Bundesmann, D. Fink, and N. Stolterfoht, *Nucl. Instrum. Methods Phys. Res. B* **232**, 235 (2005).
- [14] J. Burgdřrfer, P. Lerner, and F. W. Meyer, *Phys. Rev. A* **44**, 5674 (1991).